

Logical Filtering in Scale Space

Arjan Kuijper

Institute of Information and Computing Sciences
Utrecht University
3584 CH Utrecht, the Netherlands

Luc Florack

Department of Biomedical Engineering
Eindhoven University of Technology
NL-5600 MB Eindhoven, The Netherlands

Abstract

Using a Gaussian scale space, one can use the extra dimension, *viz.* scale, for investigation of “built-in” properties of the image in scale space. We show that one of such induced properties is the nesting of special iso-intensity manifolds, that yield an implicit present hierarchy of the critical points and regions of their influence, in the original image. Its very nature allows one not only to segment the original image automatically, but also to apply “logical filters” to it, obtaining simplified images. We give an algorithm deriving this hierarchy and show its effectiveness on two different kinds of images, both with respect to segmentation and simplification.

1 Introduction

The paradigm of linear scale space has been introduced by Witkin [28] and Koenderink [15]. They noted that a single image contains objects or parts with various sizes. One way to exploit this fact is by observing the image with filters capturing these a priori unknown sizes, or scales. Assuming that these filters should be invariant with respect to location, scale and rotations and that they should be linear, one finds the set of Gaussian filters as a plausible solution.

From the field of distribution theory [27] it is known that these filters also allow one to take derivatives up to any order of non-continuous functions, solving the question of how to define proper derivatives of a discrete set (*e.g.* an image [5]) in a well-posed way.

Nowadays, Gaussian filters are widely used to calculate derivatives of images. However, in calculating these derivatives, one needs to specify the scale, or standard deviation, of the Gaussian. One way to avoid this, is by calculating the differential properties of interest at a range of scales [7] and selecting the one with the highest (or best) response according to some pre-defined criterion.

This approaches in some sense the concept of “deep structure”, defined by Koenderink as “investigation of the image at all scales simultaneously” [15]. In essence, this implies full investigation of the n -dimensional image in $(n + 1)$ -dimensional scale space as opposed to a “slice-by-slice” approach.

Most of the research in scale space is focused on the selection of pre-defined invariants [8, 9, 12] at several scales with highest response (see e.g. [1, 24, 23, 25]). Some results have been obtained by examining the deep structure, *e.g.* in the behaviour of spatial critical points under blurring, using ideas from the field of catastrophe (or: singularity) theory [4, 6, 11, 13]. Alerted by outcome of results by Lifshitz and Pizer [22], Koenderink [16] mentioned the presence of spatial critical points in scale space with zero scale derivative and investigated their neighbourhood structure. In earlier papers [18, 20] we investigated the deep structure yielding a hierarchy tree representing the image, based on its spatial extrema at all scales, their disappearances with saddle points and the critical points in scale space found by tracing the spatial saddle points at all scales. This tree could be used to obtain a user-independent “pre-”segmentation of the image. In [19, 17] we discussed the stability of the hierarchy tree and the ability to add a priori and a posteriori known symmetry to it, and showed the effect on the pre-segmentation.

In this paper we extend the results mentioned in [18, 20] and explore the $n + 1$ dimensional scale space with respect to its critical points and its iso-intensity manifolds. We show that the latter introduce a unique hierarchy which can be used as a so-called logical filter. Consequently, a unique partitioning of the scale space is obtained, which yields, if projected to the initial image, a partitioning of the image without prior knowledge.

2 Theory

The idea of logical filtering in scale space was introduced by Koenderink in [15]. In section 2.3 we will describe this idea. In order to understand the essential elements, we firstly define a Gaussian scale space in section 2.1 and the idea of the hierarchical structure in section 2.2. The structure depends on the evolution of spatial critical points as the scale changes. The locations of these points in scale space form one dimensional manifolds, the so-called critical curves, containing two types of special points, *viz.* scale space saddles and catastrophe points.

2.1 Gaussian Scale Space

Definition 1 $L(\mathbf{x})$ denotes an arbitrary n dimensional image. We will refer to this image as the initial image. $L(\mathbf{x}; t)$ denotes the $n + 1$ dimensional Gaussian scale space image of $L(\mathbf{x})$.

The isotropic Gaussian scale space image is obtained by convolution of an initial image with a normalised Gaussian kernel:

$$L(\mathbf{x}; t) \stackrel{\text{def}}{=} G_t \star L(\mathbf{x}) \stackrel{\text{def}}{=} \int \frac{1}{\sqrt{4\pi t}^n} e^{-\frac{|\mathbf{x}-\mathbf{y}|^2}{4t}} L(\mathbf{y}) d\mathbf{y}$$

$L(\mathbf{x}; t)$ satisfies the diffusion equation:

$$\partial_t L(\mathbf{x}; t) = \sum_{i=1}^n \frac{\partial^2}{\partial x_i^2} L(\mathbf{x}; t) \stackrel{\text{def}}{=} \Delta L(\mathbf{x}; t) \quad (1)$$

Here $\Delta L(\mathbf{x}; t)$ denotes the Laplacean. Furthermore, differentiation is now well-defined, since any derivative of the image is given by the convolution of the image with the corresponding derivative of the Gaussian. The (discrete) initial image is now extended to a continuous scale space image, $L(\mathbf{x}; t) \in \mathbb{R}^n \times \mathbb{R}^+$ with $\lim_{t \downarrow 0} L(\mathbf{x}; t) = L(\mathbf{x})$.

2.1.1 Spatial critical points

Definition 2 *Spatial critical points, i.e. saddles and extrema (maxima or minima), at a certain scale t_0 are defined as the points at fixed scale t_0 where the spatial derivatives vanish: $\nabla L(\mathbf{x}; t_0) = 0$. We will refer to these points as spatial critical points to distinguish them from scale space critical points, see Definition 6.*

The type of the spatial critical points is given by the eigenvalues of the Hessian H , the matrix with the second order spatial derivatives.

Definition 3 *The Hessian matrix is defined by $H \stackrel{\text{def}}{=} \nabla \nabla^T L(\mathbf{x}; t_0)$, where each element of H is given by*

$$H_{i,j} = \frac{\partial^2}{\partial x_i \partial x_j} L(\mathbf{x}; t).$$

The trace of the Hessian equals the Laplacean. For maxima (minima) all eigenvalues of the Hessian are negative (positive). At a spatial saddle point H has both negative and positive eigenvalues.

Since $L(\mathbf{x}; t)$ is a continuously differentiable (even smooth) function in the $(\mathbf{x}; t)$ -space, spatial critical points are defined for any value t_0 and, according to the implicit function theorem, constitute a one dimensional manifold in scale space.

Definition 4 *A critical curve is a one dimensional manifold in the $(\mathbf{x}; t)$ (scale) space on which $\nabla L(\mathbf{x}; t) = 0$.*

Consequently, the intersection of all critical curves with an image at a certain scale t_0 results in the spatial critical points of the images at scale t_0 .

If at a spatial critical point the Hessian degenerates, that is: at least one of the eigenvalues is zero, the type of the spatial critical point cannot be determined using Definition 3.

Definition 5 *The catastrophe points of $L(\mathbf{x}; t)$ are defined as the points where both the spatial derivatives and determinant of the Hessian vanish: $\nabla L(\mathbf{x}; t) = 0$ and $\det H(\mathbf{x}; t) = 0$.*

In scale space the catastrophe points are isolated points and form the top of critical curves in case of annihilations, and the starting point in case of a creation. The latter requires a spatial dimension of at least two.

2.1.2 Scale Space Saddles

Definition 6 *The scale space saddles of $L(\mathbf{x}; t)$ are defined as the points where both the spatial derivatives and scale derivative vanish: $\nabla L(\mathbf{x}; t) = 0$ and $\partial_t L(\mathbf{x}; t) = 0$. Since for Gaussian scale spaces the diffusion equation holds, the latter equation equals $\Delta L(\mathbf{x}; t) = 0$.*

Note that Definition 6 describes the critical points of $L(\mathbf{x}; t)$ in scale space. In [18] it is proven that these points are always saddle points. This is a direct consequence of the notion of causality (or: the non-enhancement of local extrema, or: the prohibition of “spurious detail”, or: the maximum principle).

Definition 7 *The extended Hessian \mathcal{H} of $L(\mathbf{x}; t)$ is matrix of the second order derivatives in scale space defined by*

$$\mathcal{H} = \begin{pmatrix} \nabla\nabla^T L & \Delta\nabla L \\ (\Delta\nabla L)^T & \Delta\Delta L \end{pmatrix}. \quad (2)$$

where $\nabla\nabla^T L$ is the Hessian.

Note that in Equation (2) the elements of \mathcal{H} are purely spatial derivatives. This is possible by employing of the diffusion equation, Equation (1).

The appearance of only saddles in scale space leads to the consequence that the extended Hessian has both positive and negative eigenvalues at scale space critical points. Furthermore, in [18] we have proven that if the intensity of the spatial saddle points is parametrised by scale, the scale space saddles form the extrema of the parametrised intensity along the critical curve.

2.2 Scale Space Hierarchy

From the previous section it follows that each critical curve in $(\mathbf{x}; t)$ -space is formed by branches of critical points, where each branch is defined from a creation event or the initial scale to an annihilation event. We set $\#_C$ the number of creation events on a critical path and $\#_A$ the number of annihilation events. Since there exists a scale on which only one spatial critical point (an extremum) remains, there is one critical path with $\#_A = \#_C$, whereas all other critical paths have $\#_A = \#_C + 1$. That is, all but one critical paths are defined for a finite scale range. This widely accepted “folklore theorem” holds for L^1 -integrable images that are non-negative and have finite compact support, see Loog et al. [26].

One of the properties of scale space is the non-enhancement of local extrema. Therefore, isophotes in the neighbourhood of an extremum at a certain scale t_0 appear to move towards the extremum at coarser scale until at some scale t_1 the intensity of the extremum equals the intensity of the isophote. The extension of an isophote into scale space is called iso-intensity manifold:

Definition 8 *A iso-intensity manifold I_c , $c \in R$, is an n -dimensional manifold in $(n + 1)$ -dimensional scale space satisfying $L(\mathbf{x}; t) = c$.*

It is often implicitly understood that we consider connected components only. The iso-intensity surface in scale formed by these isophotes form a dome, with its top at the extremum.

Since the intensity of the extremum is monotonically in- or decreasing (regarding a minimum or a maximum, respectively), all these domes are nested. Retrospectively, each extremum branch carries a series of nested domes, defining increasing regions around the extremum in the input image. In [18] we have proven that these regions are closed as long as the intensity of the domes does not equal that of the dome through (the extremum and) a scale space saddle (see section 2.1.2) on the saddle branch that is connected with the extremum branch in an annihilation event. In this way a hierarchy of regions of the input image is obtained, which can be regarded as a kind of pre-segmentation. It also results in a partitioning of the scale space itself.

2.3 Logical Filtering

Since the iso-intensity manifolds are nicely nested, they can be used to form logical filters, as pointed out by Koenderink [15]: The requirement that in two “successive” derived images, say $L(\mathbf{x}; t)$ and $L(\mathbf{x}; t + \delta t)$ (with \mathbf{x} variable), corresponding points have equal illuminance and are as close as possible, yields a simple rule of *projection* between images: the orbits of the projection are the integral curves of the vector field

$$\begin{pmatrix} \dot{\mathbf{x}} \\ \dot{t} \end{pmatrix} = \begin{pmatrix} \nabla L \Delta L \\ -\|\nabla L\|^2 \end{pmatrix}. \quad (3)$$

This follows from the fact that the point $\mathbf{x} + d\mathbf{x}$ in the image at scale $t + dt$ that is connected on a iso-intensity manifold to the point \mathbf{x} at scale t , must satisfy

$$0 = \delta L = \nabla L \cdot d\mathbf{x} + \partial_t L dt = \nabla L \cdot d\mathbf{x} + \Delta L dt. \quad (4)$$

Taking the direction of steepest decent, *i.e.* in the direction of ∇L , we obtain

$$\frac{d\mathbf{x}}{dt} = -\frac{\Delta L}{\nabla L \cdot \nabla L} \cdot \nabla L$$

Noting that $\nabla L \cdot \nabla L \geq 0$, and that the singularities of the vector fields given by the Eqs. (3) and (4) coincide, namely if $\nabla L = 0$, the integral curves of the vector fields are the same.

Since the projection of a region of the image at some scale to the initial image cannot reach all points in the latter image, some regions are blanked out. These regions are described through the integral curves that pass through the extremum and those through the saddle that do reach the initial image. In Figure 6 one can see examples of iso-intensity manifolds formed by these integral curves. The region enclosed by each manifold cannot be reached. These regions are topologically equivalent to balls. Koenderink proposed to call these regions the “ranges” of the extrema, that can be taken to define the light and dark blobs defined by the extremum-saddle-point-pairs [15]. The ranges sweep out tube-like volumes, that are closed on one side. Constructing these ranges for all extrema, the image can be described as a superposition of light and

dark blobs. A sub-family may be defined for each sub-image and the original family is just the superposition of the sub-families.

We will show that the top of the tube-like volumes are found by the integral curves that pass the scale space saddles. Firstly a further investigation of the vector field Eq. (3) is presented.

3 Properties of the Vector Field

The vector field given by Eq. (3) uniquely defines integral curves, except for those points where the gradient vanishes. To investigate the local behaviour of the vector field nearby critical points, a local (Gaussian) Taylor expansion of L is used. As we will see, it suffices to take the ensemble of derivatives up to fourth order, the so-called *local jet of order 4* [8, 10]. Using the Einstein convention for repeated indices this reads

$$L^{(4)}(\mathbf{x}; t) = L_0 + L_i x^i + \frac{1}{2} L_{ij} x^i x^j + \Delta L t + \frac{1}{6} L_{ijk} x^i x^j x^k + \Delta L_i x^i t + \frac{1}{24} L_{ijkl} x^i x^j x^k x^l + \frac{1}{2} \Delta L_{ij} x^i x^j t + \frac{1}{2} \Delta \Delta L t^2. \quad (5)$$

Note that the local jet satisfies the Diffusion Equation. Locally the vector field given by Eq. (3) can be expressed by

$$\begin{pmatrix} \dot{\mathbf{x}} \\ \dot{t} \end{pmatrix} = \begin{pmatrix} v_0 \\ w_0 \end{pmatrix} + \begin{pmatrix} v_1 \\ w_1 \end{pmatrix} + \begin{pmatrix} v_2 \\ w_2 \end{pmatrix} + \dots \quad (6)$$

where the sub-indices denote the total order of the expansion in spatial variables. In terms of components we thus have

- $\begin{pmatrix} v_0^i \\ w_0 \end{pmatrix} = \begin{pmatrix} \Delta L L_i \\ -L_i^2 \end{pmatrix},$
- $\begin{pmatrix} v_1^i \\ w_1 \end{pmatrix} = \begin{pmatrix} (L_{ij} \Delta L + L_i \Delta L_j) x^j \\ -2L_i L_{ij} x^j \end{pmatrix},$
- $\begin{pmatrix} v_2^i \\ w_2 \end{pmatrix} = \begin{pmatrix} \frac{1}{2} (L_{ijk} \Delta L + 2L_{ij} \Delta L_k + L_i \Delta L_{jk}) x^j x^k + (\Delta L_i \Delta L + L_i \Delta \Delta L) t \\ -(L_{ik} L_{ij} + L_i L_{ijk}) x^j x^k - 2L_i \Delta L_i t \end{pmatrix},$
- and so on, with increasing complexity of the terms.

At spatial critical points $L_i = 0$ reducing this expansion significantly. Then the zeroth order terms vanish

- $\begin{pmatrix} v_0^i \\ w_0 \end{pmatrix} = \begin{pmatrix} 0 \\ 0 \end{pmatrix},$
- $\begin{pmatrix} v_1^i \\ w_1 \end{pmatrix} = \begin{pmatrix} (L_{ij} \Delta L) x^j \\ 0 \end{pmatrix},$
- $\begin{pmatrix} v_2^i \\ w_2 \end{pmatrix} = \begin{pmatrix} \frac{1}{2} (L_{ijk} \Delta L + 2L_{ij} \Delta L_k) x^j x^k + (\Delta L_i \Delta L) t \\ -(L_{ik} L_{ij}) x^j x^k \end{pmatrix},$

and linear terms suffice. If also the Laplacean vanishes, a further reduction of terms is established:

$$\begin{aligned} \bullet & \begin{pmatrix} v_0^i \\ w_0 \end{pmatrix} = \begin{pmatrix} 0 \\ 0 \end{pmatrix}, \\ \bullet & \begin{pmatrix} v_1^i \\ w_1 \end{pmatrix} = \begin{pmatrix} 0 \\ 0 \end{pmatrix}, \\ \bullet & \begin{pmatrix} v_2^i \\ w_2 \end{pmatrix} = \begin{pmatrix} (L_{ij}\Delta L_k) x^j x^k \\ -(L_{ij}L_{ik}) x^j x^k \end{pmatrix}. \end{aligned}$$

Consequently, a second order scheme is needed.

3.1 Local Environment

On a local environment of the vector field at critical points, reducing Eq. 6 to its first non-zero component, yields a linear system. Since $w_1 = 0$, t is constant and can be disregarded. So a linear system with only spatial coordinates remains and its behaviour is given by the scale-independent vector field

$$\dot{\mathbf{x}}^i = L_{ij}\Delta L \mathbf{x}^j. \quad (7)$$

The matrix $L_{ij}\Delta L$ in the linear system of Eq. 7 consists of two parts. The first term, L_{ij} , is equal to the Hessian matrix usually denoted by \mathbf{H} . The Laplacean term ΔL reads, apart from the scale derivative of the image, also the trace of the Hessian, since $\Delta L = L_{ii} = \text{tr}(\mathbf{H})$. At the critical curve four possibilities can occur, see Figure 1:

1. Both the trace and the determinant of the Hessian are non-zero, *i.e.* the critical point is a Morse critical point;
2. The determinant of the Hessian is zero, *i.e.* a catastrophe takes place (annihilation or creation);
3. The trace of the Hessian is zero, *i.e.* a non-topological change of the saddle;
4. Both the trace and the determinant of the Hessian are zero.

The last possibility is only generic in one-dimensional images. In higher dimensions it will therefore be disregarded.

3.2 Morse Critical Points

At Morse critical points it is convenient to reformulate Eq. 7 to

$$\dot{\mathbf{x}} = \text{tr}(\mathbf{H}) \mathbf{H} \mathbf{x} = \hat{\mathbf{H}} \mathbf{x}. \quad (8)$$

Note that the vector field given by Eq. 8 is a specially scaled extension of the usual vector field of L that is given by $\dot{\mathbf{x}} = \mathbf{H} \mathbf{x}$.

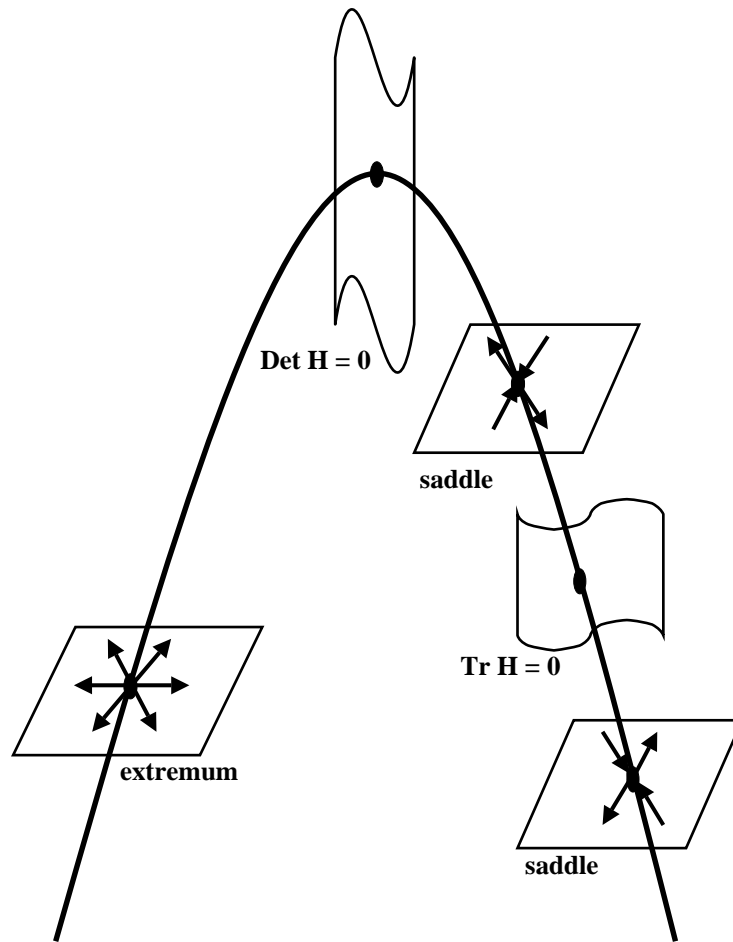


Figure 1: Possibilities of critical points in scale space on a critical curve, together with the local vector field. The left branch of the critical curve represents an extremum branch, the right one a saddle branch. Generically, critical points are somewhere on one of these branches (case 1). At the top, where $\det \mathbf{H} = 0$, a catastrophe takes place (case 2). The saddle point exhibits an extra degeneration, *viz.* where $\text{tr} \mathbf{H} = 0$ (case 3). At this point the type of saddle changes. Only in one dimensional images the cases 2 and 3 coincide generically.

The characteristics of the $\widehat{\mathbf{H}}$ vector field follows from its eigenvalues. Let (λ_i) be the set of eigenvectors of \mathbf{H} , sorted on value. Then the eigenvectors of $\widehat{\mathbf{H}}$ are given by

$$\widehat{\lambda}_i = \sum_j \lambda_j \lambda_i, \quad (9)$$

where we used $\text{tr}(\mathbf{H}) = \sum_j \lambda_j$. Consequently, away from catastrophes, saddles remain saddles and extrema remain extrema. Then the following dependencies follow straightforwardly from Eq. (9):

$$\det \widehat{\mathbf{H}} = \text{tr}(\mathbf{H})^n \det \mathbf{H}, \quad (10)$$

$$\text{tr}(\widehat{\mathbf{H}}) = \text{tr}(\mathbf{H})^2, \quad (11)$$

where n is the dimension of \mathbf{x} .

Since the trace of the Hessian equals the sum of the eigenvectors, Eq. (11) shows that all eigenvalues of $\widehat{\mathbf{H}}$ are positive definite. Consequently, the extrema of $\widehat{\mathbf{H}}$ are always minima of the vector field, *i.e.* the vectors point outward. Degenerations take place if $\det \widehat{\mathbf{H}} = 0$. According to Eq. (10) this implies the degenerations of \mathbf{H} (the catastrophe points) or the zero-crossings of the trace of \mathbf{H} .

As a result, the $\widehat{\mathbf{H}}$ vector field has only minima and corresponding saddles. When we recall the full equation of the vector field, Eq. 3, it is clear that the scale component is negative at non-critical points. The flow lines infinitesimally close to the extrema move downward in scale.

3.3 Critical Points at Catastrophes

At catastrophes, Eq. 7 loses (generically) one degree of freedom, since the Hessian becomes singular, or, to put it differently, the determinant of \mathbf{H} equals zero.

The degeneration of $\det \widehat{\mathbf{H}}$ is only caused by the vanishing determinant of \mathbf{H} ; its trace will be non-zero iff $n > 1$. Since this is generically an event of co-dimension one, also the point where $\det \widehat{\mathbf{H}}$ vanishes has also co-dimension one. The trace of $\widehat{\mathbf{H}}$ at this point is always positive definite. The argumentation of the previous section can be repeated to conclude that a catastrophe due to \mathbf{H} causes a catastrophe in $\widehat{\mathbf{H}}$. Again, while the \mathbf{H} vector field shows all sorts of catastrophes, the $\widehat{\mathbf{H}}$ vector field comprises only vector fields of catastrophes involving minima.

Consequently, at a catastrophe point the vector field of $\widehat{\mathbf{H}}$ is topologically equivalent to that of \mathbf{H} at a horseshoe surface.

3.4 Critical Points with Vanishing Laplacean

If the critical curve intersects the plane where the Laplacean of L is zero, the linear approximation Eq. 7 vanishes. A local vector field is found by examining the second order approximation of Eq. 6:

$$\begin{pmatrix} \dot{\mathbf{x}}^i \\ \dot{t} \end{pmatrix} = \begin{pmatrix} (L_{ij} \Delta L_k) x^j x^k \\ -(L_{ij} L_{ik}) x^j x^k \end{pmatrix}. \quad (12)$$

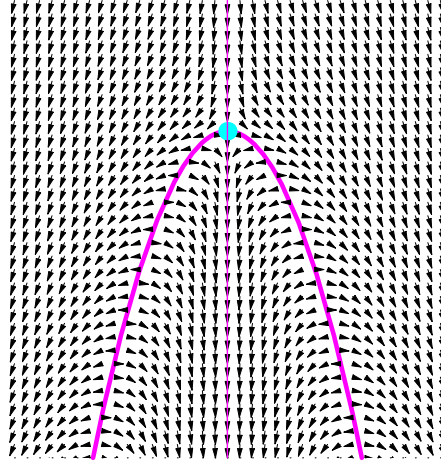


Figure 2: Vector field of a one dimensional scale space image around an annihilation at the origin, Eq. 13. The critical curve contains a catastrophe at the origin. The y -axis coincides with the zero Laplacean, reversing the spatial orientation of the vectors.

Although this expression is quite complicated, we still make the observation that a zero-Laplacean can only occur due to negative and positive eigenvalues of the Hessian, *i.e.* the critical point is always a saddle, albeit degenerate. Since the vector field involves the scale, see Eq. (12), the surface of zero-Laplacean will generically intersect the image transversally.

3.5 Non-Critical Points with Vanishing Laplacean

Although it may be clear from Eq. (3), it is emphasised that at non-critical points with zero Laplacean the vector field is non-degenerate, since it contains a non-zero scale component. If only spatial coordinates are investigated, the degeneracy is visible as a curve reversing the spatial orientation of the vectors.

3.6 Examples

3.6.1 One Dimensional Images

As already described, in one-dimensional images the determinant is equal to its trace. Therefore, at a catastrophe the critical curve also intersects the line where the Laplacean is zero. Since only annihilations occur, it suffices to investigate the generic annihilation in one dimension:

$$f(x, t) = x^3 + 6xt. \quad (13)$$

The corresponding vector field is plotted in Figure 2. The parabola is the critical curve, at its top (the origin), a minimum (the branch $x > 0$) and a maximum annihilate. As argued in section 3.2, the $\widehat{\mathbf{H}}$ -vector fields of $-f$ and f are topologically equivalent. The extrema in \mathbf{H} -vector field both become minima in the $\widehat{\mathbf{H}}$ -vector field, so the vector

field is directing away from the critical points downwardly on both sides. The line where the Laplacean is zero, *i.e.* the line $x = 0$, acts as a mirror. This follows directly from section 3.5. For $t < 0$ the zero-Laplacean is an attracting asymptote and for $t > 0$ it is a diverging one. This is caused by the change of sign on traversing the critical curve at the origin.

3.6.2 Two Dimensional Images

The generic annihilation in two dimensions is give by the function

$$f(x, t) = x^3 + 6xt + y^2 + 2t. \quad (14)$$

It contains an annihilation at the origin, and a scale space saddle at $(-1/3, 0; -1/18)$. The zero-Laplacean is given by the plane $x = -1/3$. Although this is non-generic, it suffices for our visualisation purposes.

Spatial Components of the Vector Field The vector field around Morse critical points (given by $y = 0$ and $x^2 = -2t$) for subsequent scale levels around the scale space saddle and the catastrophe point are shown in Figure 3 *for the spatial components*.

Firstly, the case for $t < -1/18$ is shown in Figure 3 top-left. On the left a typical field around a saddle is visible, on the right the same for a minimum. Between the spatial critical points the zero-Laplacean is visible as a straight line, attracting and inverting the direction of the spatial vector components.

The situation around the scale space saddle ($t = -1/18$) is shown in Figure 3 top-right, clearly showing the special second order behaviour.

The vector field for $-1/18 < t < 0$, *i.e.* between the scale space saddle and the catastrophe, is shown in Figure 3 bottom-left. Now the zero-Laplacean is diverging.

Finally, Figure 3 bottom-right shows the behaviour around the catastrophe, a combination of a saddle (on the left) and a minimum.

A Spatial and a Scale Component of the Vector Field Since the plane $y = 0$ only acts as a mirror, the situation in the (x, t) -plane is shown in Figure 4, together with the critical curve and the scale space saddle. The fact that the scale space saddle doesn't coincide with the catastrophe point forces iso-intensity manifolds that intersect the critical curve between the scale space saddle and the catastrophe point, to intersect the critical curve a second time on the right.

Obviously iso-intensity manifolds through scale space saddles form the interesting ones. In the next section we will discuss the properties of the iso-intensity manifolds.

4 Deep Structure

In this section we investigate the nature of manifolds of co-dimension 1 in scale space, form $(n + 1)$ -dimensional segments in scale space, give examples that also illustrate the definitions, and show how this route can be used to build the hierarchy embedded in the scale space image.

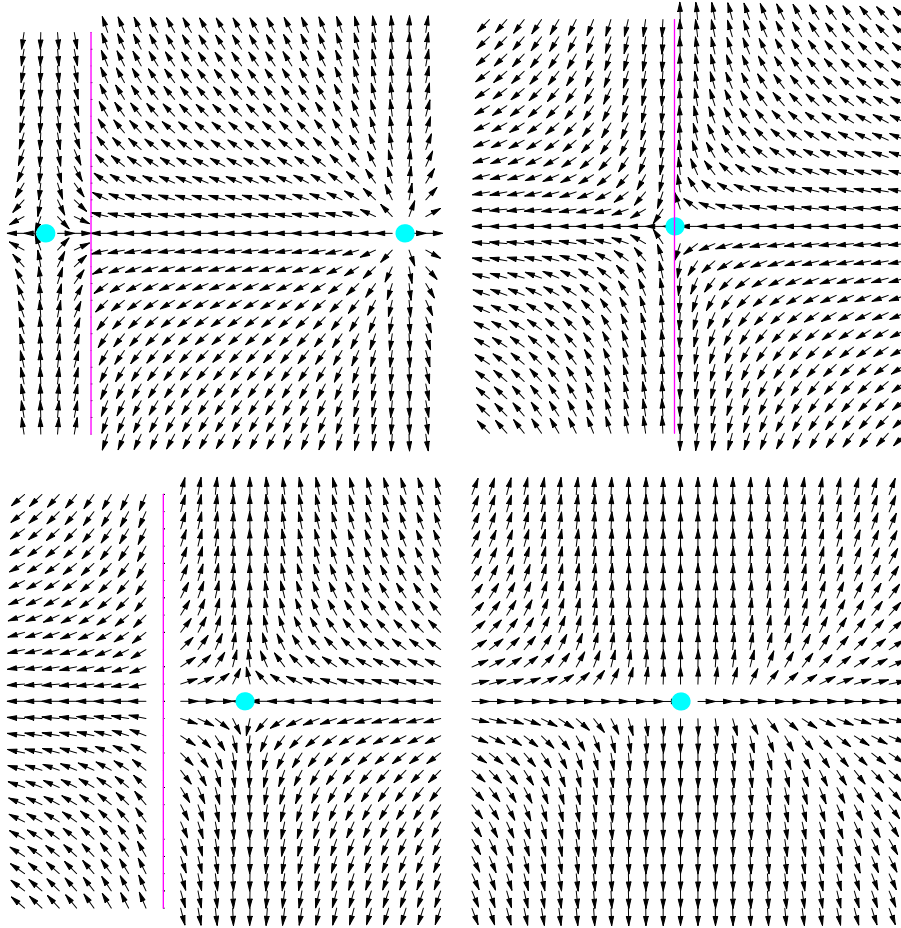


Figure 3: Vector field of the generic annihilation in two dimensions, Eq. 14, showing the *spatial* components for subsequent scale levels. The vertical line is the zero-Laplacian. Top-left: At $t < -1/18$. Top-right: At $t = -1/18$, around the scale space saddle. Bottom-left: At $-1/18 < t < 0$. Bottom-right: At $t = 0$, around the catastrophe point.

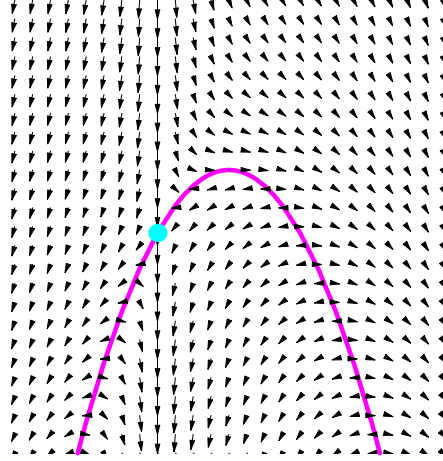


Figure 4: Vector field of the generic 2D annihilation, Eq. (14) in the $(x;t)$ plane with t vertically, together with the critical curve and the scale space saddle. At the top of the curve the two critical points annihilate.

4.1 Manifolds and Segments

Recalling Definition 8, it follows directly from Koenderink's vector field, Eq. (3) that at the top of the tube-like structure the iso-intensity manifold I_c reduces to an extremum at that scale. From Loog's argument it follows that one extremum remains, so there exist a maximum end scale at which each I_c reduces to an extremum at that scale:

Lemma 1 *Given a certain I_c , there exists exactly one point $(\mathbf{x}, \sigma) \in (\mathbb{R}^n \times \mathbb{R})$ with $L(\mathbf{x}, \sigma) \in I_c$ and $\nabla L(\mathbf{x}, \sigma) = 0$ such that $\forall \epsilon > 0 L(\mathbf{x}, \sigma + \epsilon) \notin I_c$.*

Proof of Lemma 1 *Let $(\mathbf{y}, \sigma) \in (\mathbb{R}^n \times \mathbb{R})$ and $L(\mathbf{y}, \sigma) \in I_c$. Then for all sets $((\mathbf{x}, \sigma), (\mathbf{y}, \sigma))$, the system $\mathbf{x} \neq \mathbf{y} \wedge \nabla L(\mathbf{y}, \sigma) = 0 \wedge \nabla L(\mathbf{x}, \sigma) = 0 \wedge L(\mathbf{y}, \sigma) = c \wedge L(\mathbf{x}, \sigma) = c$ yields $2n + 2$ equations with $2n + 1$ variables, and is over-determined. So necessarily $\mathbf{x} = \mathbf{y}$.*

Furthermore, let (P, S) be the set of points $(\mathbf{y}_i, \sigma_{\mathbf{y}_i}) \in (\mathbb{R}^n \times \mathbb{R})$ satisfying $\nabla L(\mathbf{y}_i, \sigma_{\mathbf{y}_i}) = 0 \wedge L(\mathbf{y}_i, \sigma_{\mathbf{y}_i}) \in I_c$. Then $\sigma_{\mathbf{y}_i} \neq \sigma_{\mathbf{y}_j}$ for $i \neq j$, and it suffices to take the point $(\mathbf{y}_i, \sigma_{\mathbf{y}_i}) \in (P, S)$ with $\sigma_{\mathbf{y}_i} = \max(S)$. \square

Obviously, there may be multiple iso-intensity manifolds with the same intensity that are disjunct in the scale space image. So the first thing to do is to relate each iso-intensity manifold to a single extremum branch. Since a single iso-intensity manifold can contain multiple extrema, but has a unique one with the highest scale, it makes sense to uniquely assign it to that extremum.

Definition 9 *A critical curve is built up of extremum and saddle branches, which are connected at catastrophe points. The set of all k extremum branches in the scale space image is given by $(e_1 \dots e_k)$.*

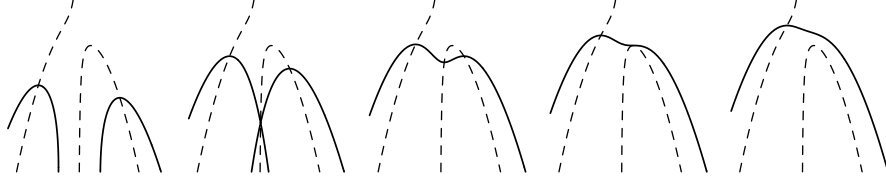


Figure 5: Critical curves (dashed curves, on the left one extremum branch e_1 , on the right a saddle branch and extremum branch e_2 , annihilating in the top point, see Definition 9) with subsequent iso-intensity manifolds (thick curves) c_1, \dots, c_5 . a) Two distinct extremum iso-intensity manifolds, see Definition 10, $I_{c_1}(e_1)$ and $I_{c_1}(e_2)$ with their top of the cones at the extremum branch. At the same time they are both extremum manifolds, see Definition 11, $M_{c_1}(e_1)$ and $M_{c_1}(e_2)$. b) The two touching extremum iso-intensity manifolds $I_{c_2}(e_1)$ and $I_{c_2}(e_2)$ are not extremum manifolds. They form the manifolds $U_{c_2}(e_1)$ and $U_{c_2}(e_2)$, see Definition 12. c) The extremum iso-intensity manifold $I_{c_3}(e_1)$ (with its top of the cone at the extremum branch e_1) is not an extremum manifold, since it intersects e_2 . d) The extremum iso-intensity manifold $I_{c_4}(e_1)$ forms the manifold $L_{c_4}(e_1)$. It touches e_2 at the annihilation point. e) The extremum iso-intensity manifold $I_{c_5}(e_1)$ is again an extremum manifold $M_{c_5}(e_1)$.

Definition 10 An extremum iso-intensity manifold $I_c(e_i)$ is the iso-intensity manifold with as global top the extremum on extremum branch e_i .

Examples of extremum iso-intensity manifolds are given in Figure 5, in which two critical curves are visualised by thick curves and five subsequent iso-intensity manifolds are drawn. It is clear that multiple types are present. To distinguish between extremum iso-intensity manifolds with multiple extrema on it, and those with only one, it is convenient to define a subset of the extremum iso-intensity manifolds:

Definition 11 An extremum manifold $M_c(e_i)$ is an extremum iso-intensity manifold intersecting of all extremum branches only the extremum branch e_i .

This type of extremum iso-intensity manifolds is shown in Figure 5a and 5e. A nesting of extremum iso-intensity manifolds is directly obtained, since the intensity of the extremum changes monotonically (either increases in case of a minimum, or decreases in case of a maximum). As a consequence, each manifold exists for a scale interval $[t_0, t_{\max}]$. Recall that there is no creation of level lines, one of the (implicit) axioms leading to the diffusion equation. Consequently, each manifold transversally intersects the initial image, cf. Koenderink's "open end of the tube-like structure". The top of this structure is located at t_{\max} : by construction the spatial extremum on the branch i forms the top of the scale space dome.

Before turning to $(n + 1)$ -dimensional segments, we first define to special types of extremum iso-intensity manifolds.

Definition 12 An upper limiting manifold $U_c(e_i)$ is an extremum iso-intensity manifold $I_c(e_i)$, such that $I_{c+\delta\epsilon}(e_i) = M_{c+\delta\epsilon}(e_i)$, $0 < \epsilon \ll 1$ and $\delta = 1$ if e_i is a maximum

and $\delta = -1$ if e_i is a minimum, but $I_c(e_i)$ is not an extremum manifold. If the maximum (minimum) branch e_i intersects n upper limiting manifolds, they are ordered on decreasing (increasing) intensity and labeled $U_{c_j}(e_i)$ for $j = 1, \dots, n$.

A lower limiting manifold $L_c(e_i)$ is an extremum iso-intensity manifold $I_c(e_i)$, such that $I_{c+\delta\epsilon}(e_i) = M_{c+\delta\epsilon}(e_i)$, $0 < \epsilon \ll 1$ and $\delta = -1$ if e_i is a maximum and $\delta = 1$ if e_i is a minimum, but $I_c(e_i)$ is not an extremum manifold. If the maximum (minimum) branch e_i intersects n lower limiting manifolds, they are ordered on decreasing (increasing) intensity and labeled $U_{c_j}(e_i)$ for $j = 1, \dots, n$.

An example is given in Figure 5. The extremum iso-intensity manifolds $U_{c_2}(e_1)$ and $U_{c_2}(e_2)$ are shown in Figure 5b. Manifolds below these two limiting manifolds (e.g. those in Figure 5a) are extremum manifolds. The extremum iso-intensity manifold $L_{c_4}(e_1)$ is shown in Figure 5d. Manifolds above this limiting manifold (e.g. the one in Figure 5e) are extremum manifolds.

The next definitions construct $(n+1)$ -dimensional segments out of the n -dimensional iso-manifolds using the two limiting manifolds.

Definition 13 *The extremum segment $E^1(e_i)$ is the volume in the scale space image under upper limiting manifold $U_{c_1}(e_i)$.*

The extremum segment $E^j(e_i)$, $j > 1$, is the volume in the scale space image under upper limiting manifold $U_{c_j}(e_i)$ and above lower limiting manifold $L_{c_{j-1}}(e_i)$.

For $0 < j < n$, $I^j(e_1)$ is the scale space volume bounded by $E^j(e_1)$ and $E^{j+1}(e_1)$.

In Figure 5, the extremum segments $E^1(e_1)$ and $E^1(e_2)$ are formed by the area beneath the manifolds $U_{c_2}(e_1)$ and $U_{c_2}(e_2)$, respectively. Note that in Figure 5, if e_1 would intersect at some intensity level c_6 a second upper limiting manifold $U_{c_6}(e_1)$, the area between $L_{c_4}(e_1)$ and $U_{c_6}(e_1)$ would also form an extremum segment, $E^2(e_2)$. Then the area between $L_{c_4}(e_1)$ and $U_{c_2}(e_1)$ forms the scale space volume $I^1(e_1)$.

So this definition yields Koenderink's tubes, but not only them. Extremum branches may intersect multiple extremum segments: From the "extremum branch point of view", starting at the initial image the branch e_i firstly intersects extremum manifolds until for some intensity c the iso-intensity manifold $I_c(e_i)$ contains a (scale space) saddle and becomes the union of two juxtaposed iso-intensity manifolds that intersect non-transversal. Note that at this point the manifold generated from e_i equals $U_c(e_i)$. Call the other part $U_c(e_j)$.

Continuing, two things can happen. The manifold $U_c(e_i) \cup U_c(e_j)$ is either $I_c(e_i)$ or $I_c(e_j)$. If the extremum branch e_i vanishes, i.e. it annihilates with the saddle branch containing the aforementioned saddle, the remaining part of the branch is no longer global top of a manifold, but part of the iso-intensity manifold $I_c(e_j)$. If it remains, e_j annihilates with intensity c_a , and the branch intersects the closed set of manifolds $[I_c(e_i), \dots, I_{c_a}(e_i)]$ and additionally again extremum manifolds. Here $I_{c_a}(e_i)$ equals $L(e_i)$ for a second extremum segment, cf. Figure 5 and the branches e_1 and e_2 .

Note that there is no third possibility, since then the iso-intensity manifold through the saddle must contain two global extrema at the same scale. This was proven to be non-generic. This observations lead to the following definition.

Definition 14 *The scale space segment $SSS(e_i)$ of an extremum branch e_i intersecting n extremum segments is*

$$SSS(e_i) = \left(\bigcup_{j=0}^n E^j(e_i) \right) \cup \left(\bigcup_{j=0}^{n-1} I^j(e_i) \right).$$

The critical manifold $C(e_i)$ is the boundary of $SSS(e_i)$.

Recalling Figure 5, the right extremum branch e_2 has one extremum segment, being the scale space segment, bounded by $U_{c_2}(e_2) = C(e_2)$. The left extremum branch has *no* scale space segment, since the second series of extremum manifolds starting above $L_{c_4}(e_1)$ is unbound. Assuming again a second upper limiting manifold $U_{c_6}(e_1)$ at intensity level c_6 , e_1 intersects two extremum segments. Then $U_{c_6}(e_1)$ forms the critical manifold $C(e_1)$. This manifold encapsulates $C(e_2)$. Then $SSS(e_2) = E^1(e_1) \cup E^2(e_1) \cup I^1(e_2)$, the complete area beneath the manifold $U_{c_6}(e_1)$ and in this example $SSS(e_2) \subset SSS(e_1)$.

By definition, $C(e_i)$ is $U_{c_n}(e_i)$, the supremum of the possible values c for which $M_c(e_i)$ exists. Since all but one extremum in the initial image annihilate with spatial saddle points, all but one extremum branch define critical manifolds. The critical manifold contains one spatial saddle, that can be located either in scale space (and thus being a scale space saddle) or at the initial image. This saddle obviously relates the extremum branch to another extremum branch, namely the one to which it is secondary in the intensity hierarchy. It is convenient to denominate this remainder of the iso-intensity manifold.

Definition 15 *Let $C(e_i) \subset I_c(e_k)$ and $(\mathbf{x}; t)$ be the saddle on $C(e_i)$. Then the dual critical manifold $D(e_i)$ is defined as*

$$\begin{aligned} D(e_i) \cup C(e_i) &= I_c(e_i), \\ D(e_i) \cap C(e_i) &= (\mathbf{x}; t). \end{aligned}$$

Note that in this definition the critical curves e_k and e_i do *not* coincide. Recalling Figure 5, $D(e_2)$ is formed by $U_{c_2}(e_1)$. In the following we will use this route to derive a unique algorithm deriving the hierarchy enclosed in the scale space image. Firstly, we will give some examples to clarify the definitions and notation.

4.1.1 Example

Consider a part of the scale space image in which a catastrophe takes place, together with a second extremum in the neighbourhood. Furthermore, take the scale range such that also a scale space saddle is present. So this part contains two critical curves, of which one contains a catastrophe point and a scale space saddle. For simplicity we assume the two extrema are maxima. Reasoning for minima is alike. An example is given in Figure 6. Note that this image is the extension of Figure 5 with an extra dimension.

The dark lines show the critical curves in scale space. The right curve contains two branches of critical points, on the left spatial saddles, on the right spatial extrema (e_r). The left curve contains an extremum curve without catastrophe points (e_l).

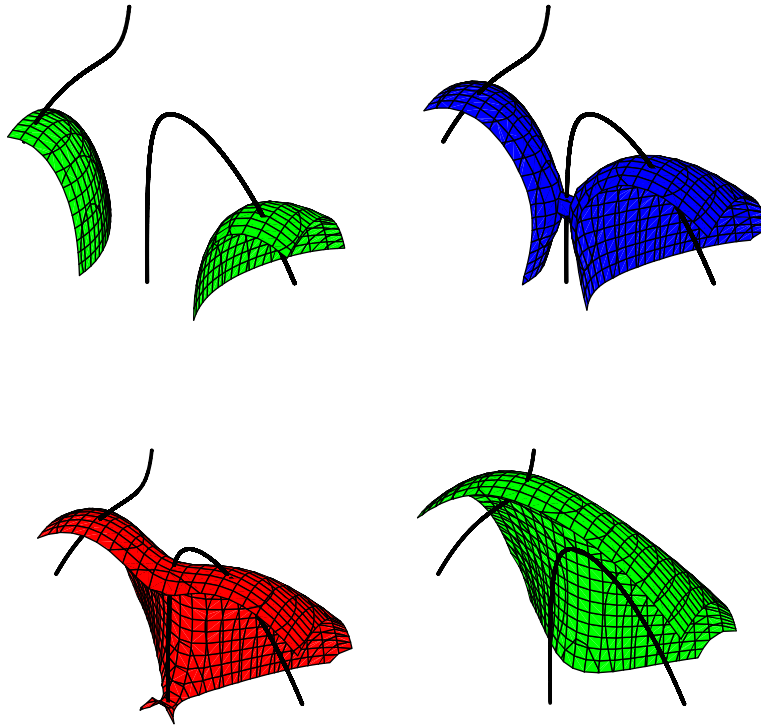


Figure 6: Subsequent iso-intensity manifolds and critical curves. Top-left: The extremum manifolds intersect the extremum branches, *cf.* Figure 5a. Top-right: The extremum iso-intensity manifolds touch at the scale space saddle, *cf.* Figure 5b. Bottom-left: The extremum iso-intensity manifold has its top on the left extremum branch, but intersects also the other extremum branch, *cf.* Figure 5c. Bottom-right: The extremum manifold intersects only the left extremum branch, *cf.* Figure 5e.

- Figure 6a shows the case with some “large” intensity c_1 . Both extremum branches intersect extremum manifolds, $M_{c_1}(e_l)$ and $M_{c_1}(e_r)$.
- Decreasing the intensity, both manifolds intersect non-transversal, as shown in Figure 6b. Now the manifolds belonging to e_l and e_r have become $U(e_l)$ and $U(e_r)$, respectively. The point of intersection is the scale space saddle. Since e_r is the vanishing extremum branch, $U(e_r)$ is defined as the critical manifold $C(e_r)$, and $U(e_l)$ is its dual $D(e_l)$. The parts enclose the extremum segments $E(e_l)$ and $E(e_r)$, respectively. The volume enclosed by $C(e_r)$, i.e. $E(e_r)$, is the scale space segment $SSS(e_r)$.
- Decreasing intensity further, the manifold has e_l as its global top, as is visible in Figure 6c. Note that although e_r still exists, there is no extremum iso-intensity manifold assigned to it. However, its influence on e_l is that for this intensity e_l is only an extremum iso-intensity manifold, and not an extremum manifold: This manifold intersects both extremum branches; also the saddle branch is intersected twice.
- This situation remains until the intensity is decreased to that of the annihilation of the right extremum. From that intensity, e_l is again an extremum manifold, as shown in Figure 6d. So the annihilation intensity forms $L(e_l)$ for a potential second extremum segment $E^2(e_l)$.

There is one scale space segment: $SSS(e_r)$. The left extremum branch doesn't define a scale space segment, since there is – in this example – no limit to the manifolds $M_c(e_l)$ for decreasing c . Only if it is assumed that this image is part of a larger image, an upper limiting manifold resulting in the segment $E^2(e_l)$, and a scale space segment $SSS(e_l)$ may be found.

It is clear that the left extremum branch contains two disjoint intensity intervals on which extremum manifolds are defined. The boundaries of these intervals are given by the intensities of the scale space saddle and the annihilation.

The nesting of the iso-intensity manifolds is shown in Figure 7.

4.1.2 A More Complicated Example

A more complicated example involving two scale space saddles and two annihilations, is visualised in Figure 8, showing the hierarchy of the two manifolds induced by the intensities c_1 and c_2 of the scale space saddles.

Again the dark lines show critical curves, from left to right extremum 1, saddle 1, extremum 2, saddle 2, and extremum 3. Extremum 2 annihilates with saddle 2, extremum 3 annihilates with saddle 1. Extremum 1 remains.

In Figure 9 the two manifolds through the scale space saddles are shown separately. In the left image, the iso-intensity manifold around e_2 and e_3 is plotted: $I_{c_1}(e_2) = I_{c_1}(e_3)$. The left part of the manifold equals $C(e_2)$, the right part $D(e_2)$. In contrast to the previous example, here also extremum e_3 annihilates, inducing another critical manifold, $C(e_3)$, shown in the right image, together with the dual $D(e_3)$.

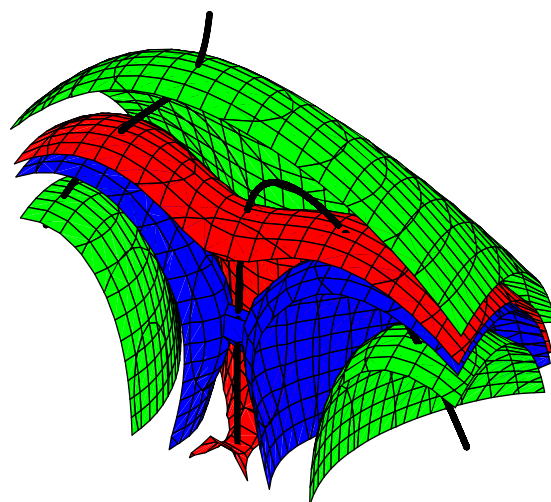


Figure 7: Nesting of iso-intensity manifolds and critical curves. See text for details.

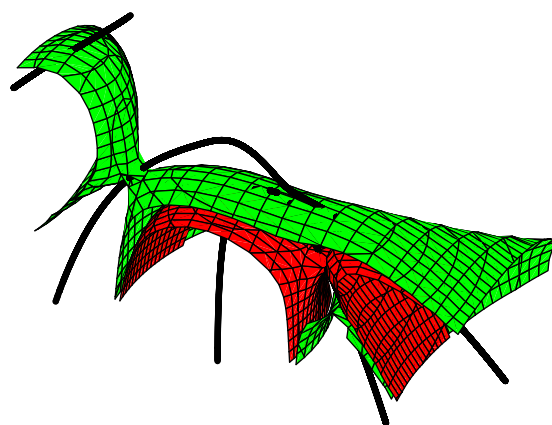


Figure 8: Iso-intensity manifolds and critical curves. See text for details.

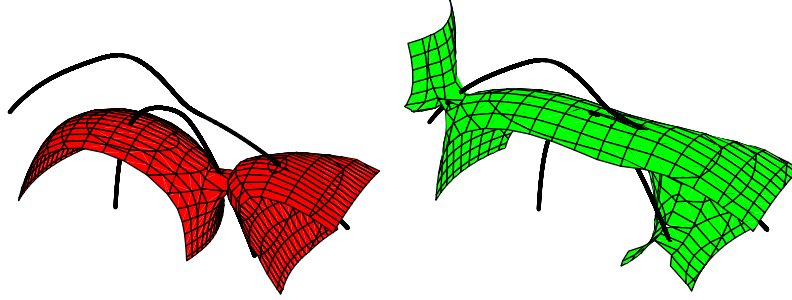


Figure 9: Iso intensity manifolds and critical curves. See text for details.

Now the critical manifold $C(e_3)$ encapsulates $I_{c_1}(e_2)$ and consequently both $C(e_2)$ and $D(e_2)$. Therefore, it may (and in this case: does) split into two disconnected spatial regions if it is traced into negative scale direction due to the intersection of the saddle branch of saddle 2. Here the scale space segment $SSS(e_3)$ exists of two connected “legs” encapsulating the extrema 2 and 3. The critical manifold $C(e_3)$ forms the “trousers” with two open ends at the initial image.

4.2 Hierarchy Algorithm

The previously described hierarchy of manifolds entails a uniquely defined description of the image, based on the critical and dual manifolds. This description is obtained by executing the following steps (that are followed by an example based on the image of the previous section):

1. Initializing:
 - (a) Build a scale space.
 - (b) Find the critical points at each scale level.
 - (c) Construct the critical branches.
 - (d) Find the catastrophe points.
 - (e) Construct and label the critical curves, including the one remaining extremum.
 - (f) Find the scale space saddles.
2. Determining the manifolds
 - (a) For each annihilating extremum e_i , find its critical iso-intensity manifold $C(e_i)$.
 - (b) Construct the dual manifolds $D(e_i)$.
3. Label to each extremum branch the dual manifolds it intersects, sorted on intensity.

4. Build a tree:
 - (a) Start with the remaining extremum at the coarsest scale as root.
 - (b) Trace to finer scale until at some value it is labeled to a dual manifold.
 - (c) Split into two branches, one the branch containing the existent extremum and assigned to the dual manifold, the other containing the extremum assigned to the critical manifold.
 - (d) Continue for all branches / extrema until all extrema are added to the tree.
5. Bonus step: return a segmentation
 - (a) Based on the binary combinations of region belonging to each defined $C(e_i)$.
 - (b) Based on the binary combinations of region belonging to each defined $C(e_i) \cup D(e_i)$.

We note that step 1 has been exploited by the authors in [18]. The other steps follow straightforwardly from the previous exercise and examples. Regarding step 3, the intensities of all extrema either increase or decrease monotonically, and so do the dual manifolds that each intersects.

The tree that is obtained is a binary tree. All annihilating extremum branches intersect a critical manifold, and each critical manifold implies a dual manifold that intersects an extremum branch underneath its own critical manifold. Therefore, all extremum branches are linked in the tree.

The creation of pairs of critical points and their influence has been dealt with elsewhere by the authors. They are not of relevance to the iso-intensity hierarchy, since scale space implies non-creation of new level lines!

As a kind of bonus, one obtains a “knowledgeless” segmentation, solely based on the hierarchy tree. This can be the concatenation of the scale space segments, or one of the scale space segments together with their dual segments.

4.2.1 Example – continued

Returning to the second example of the previous section, recall Figure 8.

1. Obviously, step 1 has been taken.
2. The algorithm yields in step 2a the two cones $C(e_2)$ and $C(e_3)$. Step 2b yields the dual cones $D(e_2)$ (intersecting e_3) and $D(e_3)$ (intersecting e_1).
3. Step 3 gives the lists $e_1 \rightarrow D(e_3)$, $e_3 \rightarrow D(e_2)$.
4. The tree is built by tracing down as root the remaining extremum, e_1 . At some scale level it intersects $D(e_3)$, so a node is added and the tree splits into two branches e_1 and e_3 . Extremum e_1 doesn’t intersect any dual manifolds and doesn’t split anymore. Extremum e_3 intersects $D(e_2)$, so a node and a new branch (e_2) is created.

Although the hierarchy dependency is obtained by the dual manifolds, we will use the critical manifolds for labeling the tree, since they identify a unique part of the scale space image to an extremum. The (binary) hierarchy tree can be collapsed into one single one-dimensional expression. The nodes of the tree are replaced by $(e_i, e_j)_{C(e_j)}$, stating that e_i is both parent and child, and e_j is child due to the fact that its dual manifold is assigned to e_i . So we have, starting at the root, firstly $(e_1, e_3)_{C(e_3)}$, and secondly the replacement of e_3 by $(e_2, e_3)_{C(e_2)}$. Consequently, the tree reduces to

$$\left(e_1, (e_2, e_3)_{C(e_2)} \right)_{C(e_3)}$$

This is to be read as “extrema 2 and 3 are related by means of the intensity of the critical manifold of extremum 2. Extremum 2 annihilates and extremum 3 is (then) related to extremum 1 by means of the intensity of the critical manifold of extremum 3”. This parentheses formula can be extended at liberty.

4.3 Visualisation and Simplification

The binary tree can easily be visualised. One way to do this, is by only displaying the scale space segments at the initial image. This has been done by the authors in [18]. A disadvantage is that the remaining extremum does not induce a scale space segment, and is thus not visible. Here we propose a visualisation strategy based on the critical manifolds together with their duals. Of both approaches we give examples.

As advantage of the latter method, now the remaining extremum is visualised. Also “more or less” symmetries appear, as we will see. Implementation is straightforward, by using a $(n + 1)$ -dimensional region growing algorithm with as seed point the saddle point connecting the critical manifold and its dual.

Simplification of the structure, or “logical filtering”, is done by sweeping out parentheses from inside to outside. Equivalently one can sweep from the leaves of the tree inwardly. The closer to the root, the more significant parts of the image are represented. The “details” are stored in the leaves ([15]). Then, for instance, example 2 could be simplified as follows:

$$\left(e_1, (e_2, e_3)_{C(e_2)} \right)_{C(e_3)} \rightarrow (e_1, e_3)_{C(e_3)}$$

That is, Figure 8 is reduced to the Figure 9b.

Note that in this hierarchy the nodes connect regions regardless of scale. For example, a small region may vanish at fine scale, but at a small intensity value. If the dual manifold encapsulates a maximum as final parent, the top of this dual dome may be achieved at very coarse scale. If it encapsulates several extrema, the logically filtered image at the initial image shows several dual regions: these dual regions necessarily encapsulate these extrema, but do not need to be connected. Examples will pop up in more realistic images in the next section.

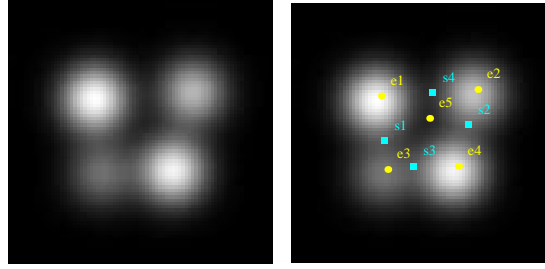


Figure 10: Left: Artificial image built by combining four maxima and one minimum. Right: Labelling of the critical points.

5 Results

The hierarchical algorithm and the possible application of logical filtering are investigated on two test images. As an artificial image allowing algebraic verification, firstly the 81×81 image is built by adding four blobs. This image is shown in Figure 10a. Secondly we used the artificial MR image Figure 14a, taken from the *Brain Web* [2, 3, 21], web site <http://www.bic.mni.mcgill.ca/brainweb>.

5.1 Blob Image

The scale space of this image was built by taking 113 scales, $e^{i/32} i = 1, \dots, 113$. The initial image contains five extrema and four saddles. One extremum, the minimum in the middle, is induced by the four extrema. Within the scale space, three scale space saddles were found: They connect cones around each vanishing extremum to the final remaining extremum. These three scale space saddles are located on saddle branches annihilating with the maximum branches. The saddle branch annihilating with the minimum branch does not contain a scale space saddle, so the value of the saddle at the initial image yields the intensity for the critical manifold encapsulating the minimum.

The labelling of the extrema and saddles is shown in Figure 10b. At coarsest scale, extremum e_4 remains. It thus forms the root. It is found that only this extremum branch belongs to dual manifolds, yielding the hierarchy tree shown in Figure 11.

The Koenderink-parentheses-formula is

$$\left(e_5, \left(e_3, \left(e_1, (e_4, e_2)_{C(e_2)} \right)_{C(e_1)} \right)_{C(e_3)} \right)_{C(e_5)}$$

Logical filtering implies firstly removing the minimum e_5 , the maximum e_3 (the least brightest), and so on.

The area in the initial image belonging to the scale space segments, encapsulated by the critical manifolds, and those encapsulated by the dual manifolds, is shown in Figure 12. Each row shows the areas encapsulated by $C(e_i)$, $C(e_i) \cup D(e_i)$, and $D(e_i)$, for $i = 1, 2, 3$ for the first, second and third row, respectively. As can be seen, e_3 yields a dual manifold containing three other extrema: the “critical intensity” of the scale space

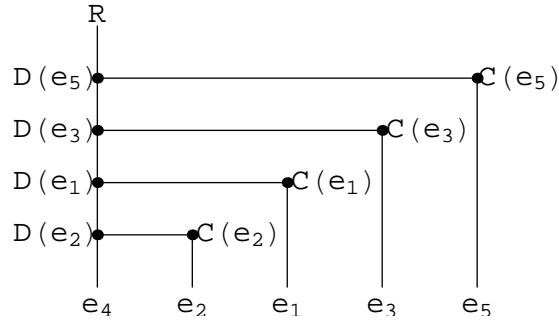


Figure 11: Hierarchy tree belonging to the artificial blob-image.

saddle is the lowest of all three scale space saddles. At increasing scale firstly $D(e_2)$ is intersected, secondly $D(e_1)$ and thirdly $D(e_3)$, as follows directly for the hierarchy tree of Figure 11.

Figure 13b shows the segmentation obtained when only the area of critical cones are plotted: the four regions belonging to the four annihilating extrema. Note that the minimum does not have a critical cone through a scale space saddle, but through the saddle at the initial image. Figure 13a extends Figure 13b by showing also the area of the dual manifolds. This elegantly shows the remaining blob e_4 , but also the hierarchy: the area around e_3 is less bright than that around e_1 , which in turn is less bright than that around e_2 and e_4 . This effect is due to the number of encapsulating dual manifolds.

5.2 MR Image

The MR image, shown in Figure 14a, contains 812 extrema. For visualisation purposes we take as initial scale $t = 8.39$, yielding the image shown in Figure 14b.

This image contains 7 extrema, as labelled in the image. The scale space image in the scale range $t \in (8.39, 33.1)$ is exponentially sampled by 89 scales. This yields the following annihilating couples: (e_1, s_3) , (e_2, s_2) , (e_3, s_4) , (e_5, s_6) , (e_6, s_1) , and (e_7, s_5) . On the saddle branches of the saddles s_1, s_2, s_3, s_5 scale space saddles are found. The saddle branches s_4 and s_6 have their global extremal intensity at the initial scale (8.39). The intersections of the image at scale $t = 8.39$ and the manifolds $C(e_i)$ and $D(e_i)$ for $i \in [1, \dots, 7]$ (except, of course, e_4) are shown in Figure 15, labelling from left to right, top to bottom. Note that the critical manifold and its dual can appear both juxtaposed and nested. The top row represents the regions belonging to the maxima in the initial image, the bottom row to the minima.

The labelling of extrema to dual manifolds gives the following sequences:

$$\begin{aligned} e_4 &\rightarrow \{D(e_6), D(e_2), D(e_3)\} \\ e_6 &\rightarrow \{D(e_7), D(e_5)\} \\ e_2 &\rightarrow \{D(e_1)\} \end{aligned}$$

The hierarchy tree belonging to it is shown in Figure 16.

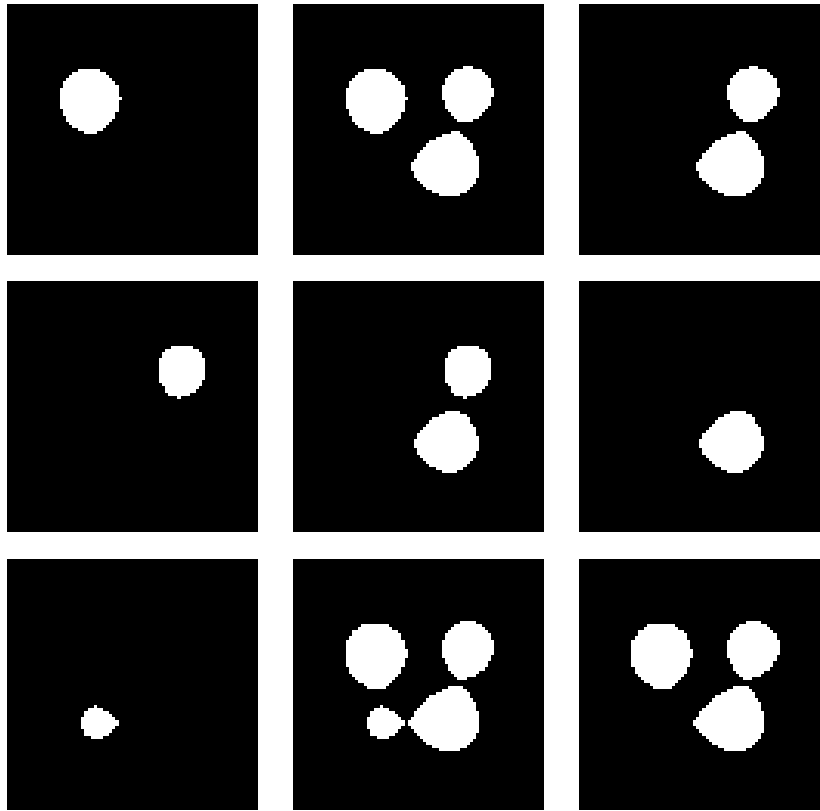


Figure 12: Each row: Regions at the initial image encapsulated by the following manifolds for $i = 1$ (top row), $i = 2$ (middle row), and $i = 3$ (bottom row): Left: $C(e_i)$, Middle: $C(e_i) \cup D(e_i)$, Right: $D(e_i)$.

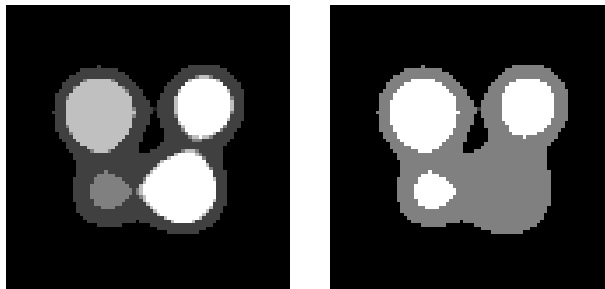


Figure 13: Left: Segmentation based on the binary combinations of region belonging to each defined $C(e_i) \cup D(e_i)$, $i \in [1, \dots, 5]$. Right: Segmentation based on the binary combinations of region belonging to each defined $C(e_i)$, $i \in [1, \dots, 5]$.

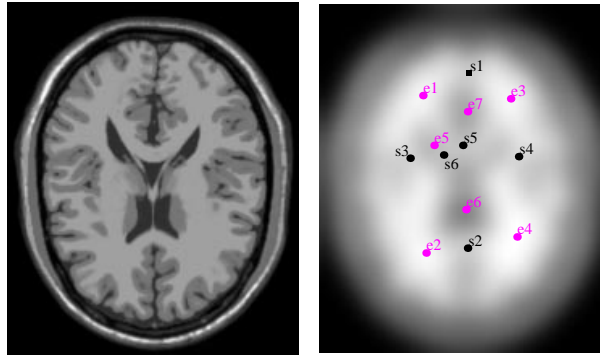


Figure 14: Left: 181 x 217 artificial MR image. Right: MR image at scale $t = 8.37$.



Figure 15: Contours of the critical and dual manifolds at the MR image at scale 8.39. Top row: Left) $C(e_1)$ (lower contour) and $D(e_1)$. Middle) $C(e_2)$ (left contour) and $D(e_2)$. Right) $C(e_3)$ (upper part of the contour) and $D(e_3)$. Bottom row: Left) $C(e_5)$ (top left part of the contour) and $D(e_5)$. Middle) $C(e_6)$ (inner contour) and $D(e_6)$. Right) $C(e_7)$ (small circle) and $D(e_7)$.

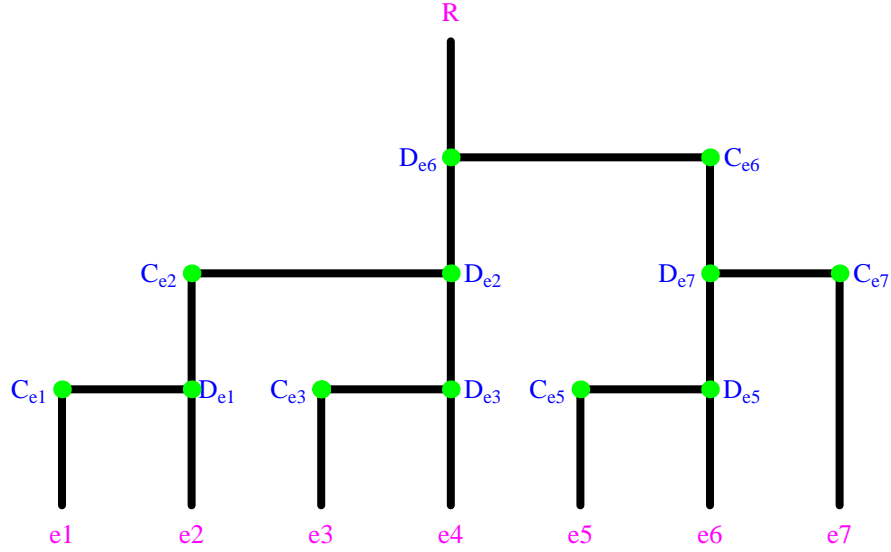


Figure 16: Hierarchy tree for the MR image.

The corresponding segmentation based on the binary combinations of region belonging to each defined $C(e_i) \cup D(e_i), i \in [1, \dots, 7]$ is shown in Figure 17a. The close nesting of the intersection manifolds is visualised in Figure 17b. This suggests that for the sake of a “meaningful” segmentation, certain extrema are less important than others, or even redundant altogether. Taking into account all extrema may in some sense result in an “over-segmentation”.

One target for logical filtering could be identifying all minima regions and all maxima regions. For the tree this would imply removing the leaves e_5, e_7 and e_1, e_2, e_3 , respectively. The parentheses formulation is simplified from

$$\left(\left((e_1, e_2)_{C(e_1)}, (e_3, e_4)_{C(e_3)} \right)_{C(e_2)}, \left((e_5, e_6)_{C(e_5)}, e_7 \right)_{C(e_7)} \right)_{C(e_6)} \quad (15)$$

via (for example!)

$$\left((e_2, e_4)_{C(e_2)}, (e_6, e_7)_{C(e_7)} \right)_{C(e_6)} \quad (16)$$

to

$$(e_4, e_6)_{C(e_6)} \quad (17)$$

This sequence of simplification is visualised in Figure 17. The top row shows the simplification of the binary combinations of regions belonging to selected manifolds, the bottom row shows the involved isophotes (intersections of the manifolds with the images at scale 8.37). The left couple of Figure 17 visualise Eq. (15). The first reduction of Eq. (16) is shown by the middle pair of images of Figure 17. The final simplification of Eq. (17) yields the right set of images in Figure 17. This illustrates the remark on “redundancy” quite neatly.

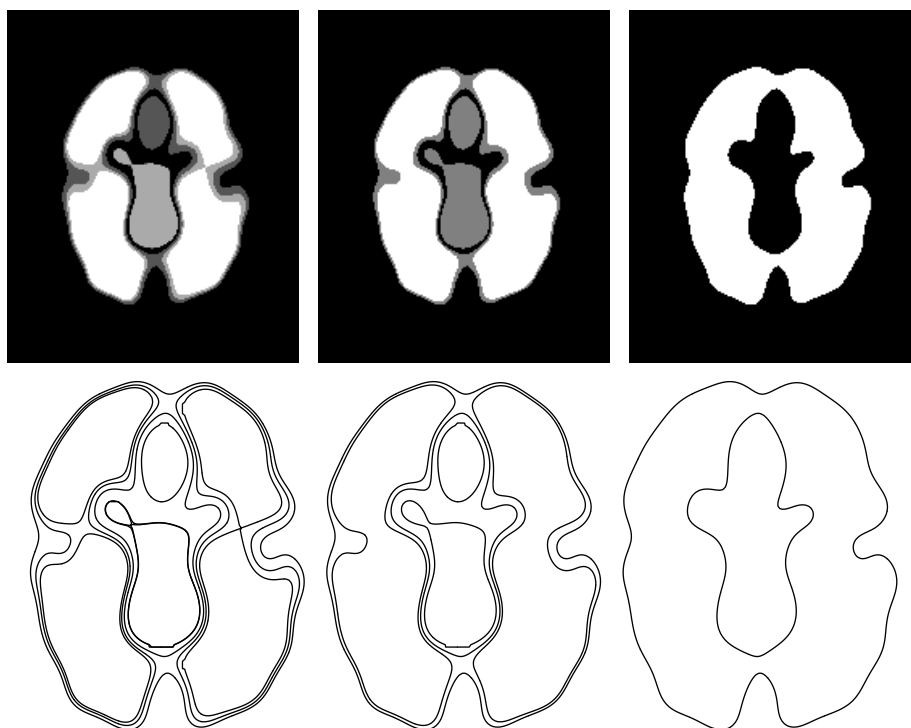


Figure 17: Example of logical filtering. Top row: Segmentation based on the binary combinations of region belonging to each defined $C(e_i) \cup D(e_i)$, from left tot right according to a) Eq. (15), b) Eq. (16), c) Eq. (17). Bottom row, d-f): Nesting of the corresponding contours as shown in the top row

6 Summary and Discussion

In this chapter we investigated the deep structure of Gaussian scale space. A scale space image is obtained by convolution of an initial image with a normalised Gaussian with variable width, or scale. We showed that the critical curves, obtained when increasing scale, provide useful information for deriving a hierarchy structure that solely depends on intrinsic entities of the scale space.

Firstly, we investigated the mathematical properties of the vector field proposed by Koenderink. We showed that its characteristic behaviour is well-defined on all non-critical points. On Morse critical points a linear expansion suffices to derive the local vector field. It is *always* topologically equivalent to a vector field containing only minima (source nodes) and corresponding saddles. Non-Morse critical points are separated into two groups in n -D images, $n > 1$, namely those where the determinant of the Hessian vanishes (catastrophe points) and those where the Laplacean is zero (scale space saddles). The first group can easily be evaluated, the second group is more difficult to examine and the structure of iso-intensity contours through them gives more insight in the local structure around these points. In one dimensional images these groups coincide. It appears that the vector field proposed by Koenderink is a powerful tool in understanding the structure of an image at all levels of resolution simultaneously.

Secondly, we investigated the properties of the manifolds obtained by the integral curves of the vector field. We showed that to each extremum uniquely a scale space segment can be assigned. To this segment a natural extension can be made by means of its “dual” segment. Both segments have an manifold of co-dimension one as boundary with the same intensity. Their intersection contains one point, either a scale space saddle with the scale space image, or a spatial saddle point in the initial image. The maximum (or causality) principle guarantees that all iso-intensity manifolds in scale space behave proper, *i.e.* they are nicely nested and, they form surfaces that are closed above (at high scale) and have open ends in the initial image. No new manifolds are created upon coarsening.

The dual manifold, as boundary of the dual segment, provides the information needed for automatic building a (binary) hierarchy tree, that can be represented as a nested sequence (parentheses formulation) of related extrema and their linking saddle. This reduced representation of the image allows one to “filter logically”. Parts of the tree, or sub-parentheses structures can be filtered out. It merely boils down to filter out certain preselected parts of the image.

We gave a theoretical expose to derive a self explanatory algorithm. This algorithm was applied to two test images, showing the usefulness of the conceptual ideas behind it.

Again we emphasise that the structure obtained is without any a priori information and is solely derived from the fact that convolution with a Gaussian (as test, or regularisation function in mathematical sense) is necessary in order to be able to perform well-defined continuous operations on a discrete image. The proposed hierarchy is thus induced by this mathematical concept.

As possible applications one can think of – besides of course user-independent segmentation and image simplification – image storage using compressed information, transmission by means of “significant data first”, image comparison, both searching in

databases as stereo images, and so on.

References

- [1] O. Chomat, V. Colin de Verdière, and J. L. Crowley. Recognizing goldfish? or local scale selection for recognition techniques. *Robotics and Autonomous Systems*, 35:191–200, 2001.
- [2] C. A. Cocosco, V. Kollokian, R. K.-S. Kwan, and A. C. Evans. Brainweb: Online interface to a 3D MRI simulated brain database. In *NeuroImage, vol.5, no.4, part 2/4, S425, 1997 – Proceedings of 3-rd International Conference on Functional Mapping of the Human Brain, Copenhagen, May, 1997*.
- [3] D. L. Collins, A. P. Zijdenbos, V. Kollokian, J. G. Sled, N. J. Kabani, C. J. Holmes, and A. C. Evans. Design and construction of a realistic digital brain phantom. *IEEE Transactions on Medical Imaging*, 17(3):463–468, 1998.
- [4] J. Damon. Generic structure of two-dimensional images under Gaussian blurring. *SIAM Journal on Applied Mathematics*, 59(1):97–138, 1998.
- [5] L. M. J. Florack. *Image Structure*, volume 10 of *Computational Imaging and Vision Series*. Kluwer Academic Publishers, Dordrecht, The Netherlands, 1997.
- [6] L. M. J. Florack and A. Kuijper. The topological structure of scale-space images. *Journal of Mathematical Imaging and Vision*, 12(1):65–80, February 2000.
- [7] L. M. J. Florack, B. M. ter Haar Romeny, J. J. Koenderink, and M. A. Viergever. Scale and the differential structure of images. *Image and Vision Computing*, 10(6):376–388, July/August 1992.
- [8] L. M. J. Florack, B. M. ter Haar Romeny, J. J. Koenderink, and M. A. Viergever. Cartesian differential invariants in scale-space. *Journal of Mathematical Imaging and Vision*, 3(4):327–348, 1993.
- [9] L. M. J. Florack, B. M. ter Haar Romeny, J. J. Koenderink, and M. A. Viergever. General intensity transformations and differential invariants. *Journal of Mathematical Imaging and Vision*, 4(2):171–187, May 1994.
- [10] L. M. J. Florack, B. M. ter Haar Romeny, J. J. Koenderink, and M. A. Viergever. The Gaussian scale-space paradigm and the multiscale local jet. *International Journal of Computer Vision*, 18(1):61–75, April 1996.
- [11] L. D. Griffin and A. Colchester. Superficial and deep structure in linear diffusion scale space: Isophotes, critical points and separatrices. *Image and Vision Computing*, 13(7):543–557, September 1995.
- [12] B. M. ter Haar Romeny, L. M. J. Florack, A. H. Salden, and M. A. Viergever. Higher order differential structure of images. *Image and Vision Computing*, 12(6):317–325, 1994.

- [13] S. N. Kalitzin, B. M. ter Haar Romeny, and M. A. Viergever. On topological deep-structure segmentation. In *proceedings of ICIP'97, Santa Barbara*, volume II, pages 863–866, 1997.
- [14] M. Kerckhove, editor. *Scale-Space and Morphology in Computer Vision*, volume 2106 of *Lecture Notes in Computer Science*. Springer -Verlag, Berlin Heidelberg, 2001.
- [15] J. J. Koenderink. The structure of images. *Biological Cybernetics*, 50:363–370, 1984.
- [16] J. J. Koenderink. A hitherto unnoticed singularity of scale-space. *IEEE Transactions on Pattern Analysis and Machine Intelligence*, 11(11):1222–1224, 1989.
- [17] A. Kuijper and L. M. J. Florack. The application of catastrophe theory to image analysis, 2001. submitted.
- [18] A. Kuijper and L. M. J. Florack. Hierarchical pre-segmentation without prior knowledge. In *Proceedings of the 8th International Conference on Computer Vision (Vancouver, Canada, July 9–12, 2001)*, pages 487–493, 2001.
- [19] A. Kuijper and L. M. J. Florack. Understanding and modeling the evolution of critical points under Gaussian blurring. In *Proceedings of the 7th European Conference on Computer Vision (Copenhagen, Denmark, May 28–31, 2002)*, pages ..–., 2002.
- [20] A. Kuijper, L. M. J. Florack, and M. A. Viergever. Scale space hierarchy, 2001. accepted for publication.
- [21] R. K.-S. Kwan, A. C. Evans, and G. B. Pike. An extensible MRI simulator for post-processing evaluation. In *Visualization in Biomedical Computing (VBC'96). Lecture Notes in Computer Science, vol. 1131. Springer-Verlag, pages 135-140, 1996.*
- [22] L. M. Lifshitz and S. M. Pizer. A multiresolution hierarchical approach to image segmentation based on intensity extrema. *IEEE Transactions on Pattern Analysis and Machine Intelligence*, 12(6):529–540, 1990.
- [23] T. Lindeberg. Edge detection and ridge detection with automatic scale selection. *International Journal of Computer Vision*, 30(2):117–154, 1998.
- [24] T. Lindeberg. Feature detection with automatic scale selection. *International Journal of Computer Vision*, 30(2):79–116, 1998.
- [25] T. Lindeberg. A scale selection principle for estimating image deformations. *Image and Vision Computing*, 16:961–977, 1998.
- [26] M. Loog, J. J. Duistermaat, and L. M. J. Florack. On the behavior of spatial critical points under Gaussian blurring, a folklore theorem and scale-space constraints. In *Kerckhove [14]*, pages 183–192, 2001.

- [27] L. Schwartz. *Théorie des Distributions*, volume I, II of *Actualités scientifiques et industrielles; 1091,1122*. Publications de l'Institut de Mathématique de l'Université de Strasbourg, Paris, 1950–1951.
- [28] A. P. Witkin. Scale-space filtering. In *Proceedings of the Eighth International Joint Conference on Artificial Intelligence*, pages 1019–1022, 1983.